

# Journal of Materials Chemistry A

Accepted Manuscript



This is an *Accepted Manuscript*, which has been through the Royal Society of Chemistry peer review process and has been accepted for publication.

*Accepted Manuscripts* are published online shortly after acceptance, before technical editing, formatting and proof reading. Using this free service, authors can make their results available to the community, in citable form, before we publish the edited article. We will replace this *Accepted Manuscript* with the edited and formatted *Advance Article* as soon as it is available.

You can find more information about *Accepted Manuscripts* in the [Information for Authors](#).

Please note that technical editing may introduce minor changes to the text and/or graphics, which may alter content. The journal's standard [Terms & Conditions](#) and the [Ethical guidelines](#) still apply. In no event shall the Royal Society of Chemistry be held responsible for any errors or omissions in this *Accepted Manuscript* or any consequences arising from the use of any information it contains.

**A highly flexible and substrate-independent self-powered deformation sensor based on massively aligned piezoelectric nano-/microfibers**

Yiin-Kuen Fuh<sup>1</sup>, Jia-Cheng Ye<sup>2</sup>, Po-Chou Chen<sup>3</sup>, Zih-Ming Huang<sup>3</sup>

<sup>1</sup>*Department of Mechanical Engineering, National Central University, No.300,*

*Jhongda Rd., Zhongli City, Taoyuan County 32001, Taiwan (R.O.C.)*

<sup>2</sup>*Energy Engineering, National Central University, No.300, Zhongda Rd., Zhongli City,*

*Taoyuan County 32001, Taiwan (R.O.C.)*

<sup>3</sup>*Mechanical Engineering, National Central University, No.300, Zhongda Rd., Zhongli*

*City, Taoyuan County 32001, Taiwan (R.O.C.)*

**Corresponding author:** Dr. Yiin-Kuen Fuh

**Mailing Address:** Department of Mechanical Engineering, National Central

University, No.300, Zhongda Rd., Zhongli City, Taoyuan County 32001, Taiwan

(R.O.C.)

**Telephones:** +886- 03-4267305 (office)

**Fax:** +886- 03-4254501

**E-mail:** [michaelfuh@gmail.com](mailto:michaelfuh@gmail.com)/[stuvwxyz0618@gmail.com](mailto:stuvwxyz0618@gmail.com)

**Abstract:**

In this study, we demonstrate highly flexible and substrate-independent piezoelectric nano-/microfiber (NMF) arrays that have the potential to function as a self-powered active deformation sensor. The fabricated hybrid structure of sensor/power generator (PG) is realized via direct deposition of near-field electrospun and in-situ poled polyvinylidene fluoride (PVDF) NMF on Cu-foil electrode of thickness  $\sim 200$   $\mu\text{m}$ . NMF-based active deformation sensor has been successfully deposited on four different flexible substrate materials including paper and fully encapsulated with comparable electrical output performance, demonstrating the superior functionality of substrate-independent deposition of NMF arrays. Capable of integrating into fabric such as a waving flag due to its high flexibility and excellent conformability, the NMF-based device can serve as an active deformation sensor under ambient wind-speed and the feasibility of efficiently converting the flutter motion into electricity are also demonstrated. This low-cost, simple structure, high sensitivity and good environment-friendly NMF based PG is a very promising material/technology for practical energy harvesting devices and self-powered sensors and capable of scavenging very small wind power or mechanical induced vibration.

**1. Introduction**

Renewable and green energy resources such as wind and solar power have considerably rekindled intensive interest to circumvent the energy crisis and global warming. In addition, self-powered micro/nanosystems and energy harvesting technologies, based on the piezoelectric effect of zinc oxide (ZnO) nanowires (NWs), have been widely developed for converting very small-scale mechanical energy to electricity<sup>1-6</sup>. The first significant contribution dates back to 2006, at which time via piezoelectric effect a single ZnO NW was demonstrated to convert nanoscale mechanical energy into electrical energy. A conductive atomic force microscope tip in contact mode was used to deflect aligned NWs and  $\sim 8\text{mV}$   $\sim 0.5$  pW were generated from a single NW actuation<sup>7</sup>. A piezoelectric nanogenerator (NG) based on lead zirconate titanate (PZT) NWs was presented such that the measured output voltage and power under periodic stress application was 1.63 V and 0.03  $\mu\text{W}$ <sup>8</sup>. Another recent development in new nanomaterial system is to utilize BaTiO<sub>3</sub> nanotubes as synthesized by the hydrothermal method and the peak open-circuit voltage and short-circuit current of the NG has reached a high level of 5.5 V and 350 nA, respectively.<sup>9</sup> For both nanomaterials systems, a specific and sophisticated nano-assembly step is required and PZT NWs also needs additional high temperature sintering and post-poling steps. Therefore, a direct-write polyvinylidene fluoride

(PVDF) nano-/microfiber (NMF) with high energy conversion efficiency has been proposed to overcome the above issues and realize electrical outputs of 5 - 30 mV and 0.5 - 3 nA for a single NMF<sup>10</sup>. The direct-write capability can only be possible due to the near-field electrospinning (NFES) that has highly controllable and patterning capabilities to deposit solid nanofibers (NFs) in a direct, continuous, and controllable manner<sup>11</sup>. Controlled complex patterns such as circular shapes and grid arrays on large and flat areas can be obtained<sup>12</sup>. Ambient vibration resources have the characteristics of variable frequencies and amplitudes. Many kinds of NGs have been demonstrated to harvest very small-scale mechanical resources such as light wind, body movement, vibrations and acoustic/ultrasonic waves<sup>13-17</sup>. For the latest comprehensive review on self-powered micro/nano-technology<sup>23</sup> and recent progress of nanodevices in self-powered active sensor array<sup>24</sup>, the key is to develop a fully functional system to facilitate the transformation of nanoscale science into applicable nanotechnology. More specifically, NGs based active sensors have been developed such as heart-pulse<sup>18</sup>, tire pressure<sup>19</sup>, vortex capture detection<sup>20</sup> and respiration<sup>21</sup>. Furthermore, a recent study successfully employed massively parallel aligned microfibers-based harvester deposited via in situ, oriented poled NFES with a unique polarity alignment and a total of 500 microfibers continuously deposited in parallel and serial configurations, which are capable of producing a peak output voltage of  $\sim 1.7$  V and current of  $\sim 300$  nA. This development has made the self-powered NMF-based PG a step further towards the actual deployment<sup>22</sup>. For a wide variety of applications, power generators (PGs) with high flexibility is essential for energy harvesting and sensor devices. We report a direct-write and in-situ poled PG via NFES process to deposit polymeric PVDF NMF arrays fully encapsulated on a flexible substrate. Cost-effective thin metallic electrodes enable energy harvesting such that the packaged device was able to easily flutter with high-amplitude of vibration under low-speed air flow ( $\approx 3.4$  m/s) and the vibration frequency was over 5 Hz. Furthermore, the same device was utilized and demonstrated as a simple and inexpensive deformation sensor for fluttering motion measurement. The proportional correlation between output current/voltage and wind speed was also obtained, and the measured maximum outputs were over 100 nA and 2.5 V, respectively for the wind speed 11.3 m/s. Moreover, the NMF-based PG has the advantages of five-fold increased voltage/current outputs as compared with ZnO NW- based PG.

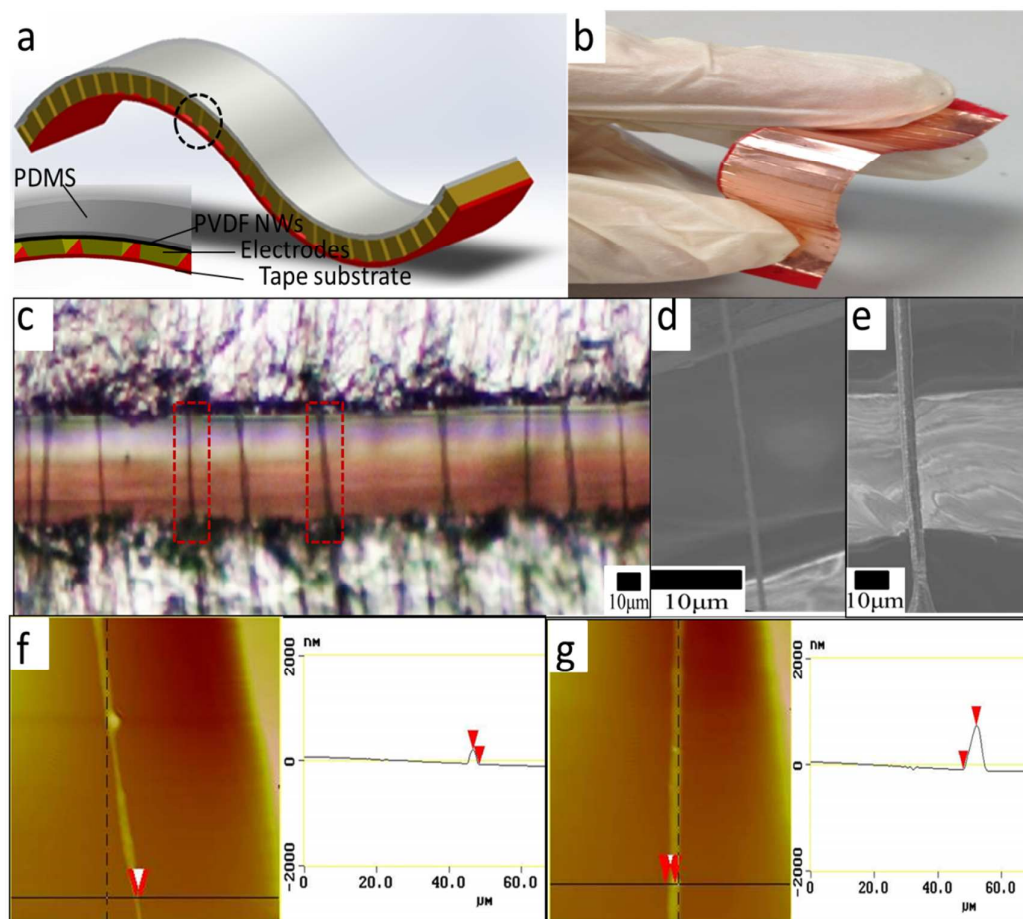


Figure 1 NMF-based PG design, fabrication and characterization. (a) Schematic diagram of the PG design. (b) Digital photo of the fabricated PG. (c) Optical images of a fabricated device with parallel aligned NMF. The working gap between two electrodes was  $\sim 50\mu\text{m}$ . (d) Enlarged SEM micrograph showing NMF with diameter of  $\sim 2\mu\text{m}$  (e) Enlarged SEM micrograph showing NMF with diameter of  $\sim 4\mu\text{m}$ . All scale bars were  $10\mu\text{m}$ . (f-g) Atomic Force Microscope (AFM) images of PVDF NMF of two different diameters fabricated via direct-write NFES technique. The continuous deposition of PVDF NMF poses a severe challenge and a very narrow operating region was identified, at the sacrifice of diameter variation of NMF.

## 2. Direct-write, in-situ poled NMF-based PG

Originally, the PG was invented for creating self-powered systems and supporting sensor networks. In this work, we propose a three-layer structure based on direct-write NMF to achieve high power output and high sensitivity, as shown schematically in Figure 1a. The working principle and structure of the PG was comprised of electrospun PVDF NMF in a fashion of direct-write, parallel aligned and in-situ poled on a flexible substrate. The aligned dipoles were necessary since electrical potentials can only be generated under dynamic strain/stress by bending the flexible substrate. The physical stability of the entire structure was maintained by encapsulating a thin layer of insulating poly(dimethylsiloxane) (PDMS) inside. Figure 1b shows an optical image of PG with significant bending flexibility. Highly flexible topology was critical for energy harvesting devices or active sensors, since for practical use in environments, the available dynamic strain/stress induced motion and shape cannot be confined precisely. The size of the fabricated PG was  $65\text{ mm} \times 15\text{ mm} \times 0.65\text{ mm}$ . Encapsulation of PDMS was applied to ensure structural stability. A total of about 50 parallel NMF have been electrospun on top of the 25 metallic electrodes with the working gap between two electrodes was  $\sim 50\mu\text{m}$ . This is shown in Figure 1c. When dynamic strain/stress was applied by bending the flexible substrate, there were about 1250 active working contacts to collect charges generated from these PVDF NMF. The as-spun PVDF NMF have diameters ranging from 900 nm to  $5\mu\text{m}$ . Figures 1d-e show the scanning electron microscope (SEM) images of two PVDF NMF fabricated via direct-write NFES processing conditions. Due to the spinnability of PVDF solution, the continuous deposition of PVDF NMF poses a severe challenge and a very narrow operating region was identified in this research, at the sacrifice of diameter variation of NMF. We have intentionally chosen the most notably different diameters of NMF and performed the characterization. The corresponding AFM images are shown in Figure 1f-g, indicating the diameter is  $\sim 1.7\mu\text{m}$  and  $4.1\mu\text{m}$ . One key contribution of this work is the experimental validation on the spinnability of NFES PVDF NMF. In order to facilitate the continuous and large-area deposition, the NFES spinning window was experimentally identified for PVDF solution, which was relatively narrow compared to other commonly used solution such as poly(ethylene oxide)(PEO). The distinctive feature of the proposed direct-write PG/self-powered sensor is the favorably substrate-independent deposition of NMF arrays. Four different flexible substrates of PVC, Kapton, Cellulose paper and insulating tape have been successfully deposited with comparable performance as shown in Supplementary information Figure S1. The mechanism and detailed explanation on the in situ mechanical stretching and electrical poling during direct-write technique by means of NFES can be found in Supplementary information Figure S2.

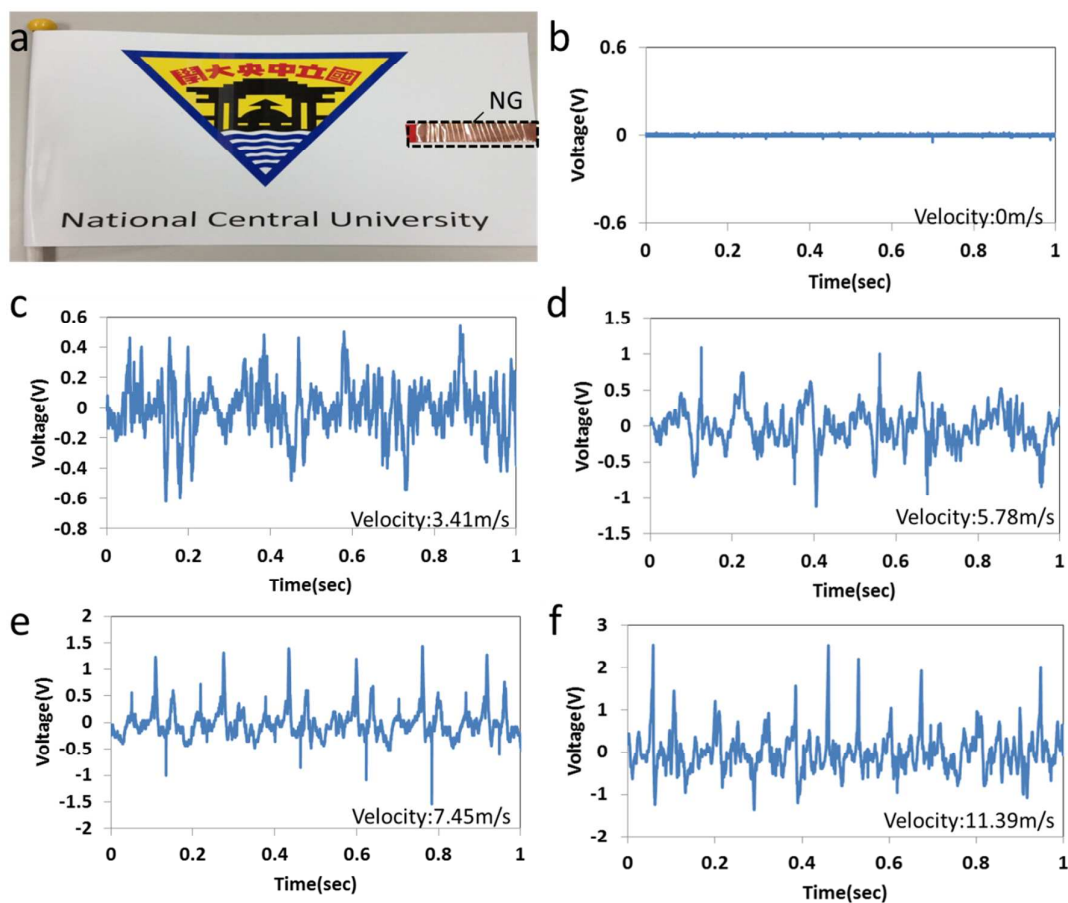


Figure 2 A wind energy harvesting device with voltage outputs under various air-flow velocities. (a) Schematic diagram of experiment for voltage measuring at wind speed of (b) 0 m/s. (c) 3.41 m/s. (d) 5.78 m/s. (e) 7.45 m/s. (f) 11.39 m/s, respectively.

### 3. PG of the fluttering motion

Figure 2a shows optical images of a fabricated PG device based on direct-write electrospun NMF and bonded firmly on top of the flag surface with glue. In order to simulate the ambient wind condition and simultaneously achieve a controllable and steady air flow, the flag was first placed in a calm indoor environment and compressed air was introduced with an electric fan. An electric fan with an inner diameter of 50mm was placed in front of the PG-bonded flag to activate the parallel

air flow. The flow velocity through the flag was measured with a commercial wind meter (TES-1340). Figure 2b shows the input air-flow velocity of 0 m/s and the corresponding voltage output. Experimentally, the output voltage was in the range of -30 to 15mV. A 60 Hz background noise from system interference was filtered out in the subsequent measurements. Figures 2c-f show the outputs of the PG harvester at different velocities which was the result of the fluttering motion. Fast Fourier transform (FFT) was used to identify the frequencies from voltage outputs and is listed in Table 1. It was observed that the frequency increases noticeably with the increase of the air-flow velocity. FFT calculated frequencies were 5, 17, 22 and 50Hz when air-flow velocities were 3.41, 5.78, 7.45, and 11.39m/s, respectively. A cubic polynomial was data-fitted as  $v = -8 \times 10^{-5}f^3 + 0.0042f^2 + 0.1588f + 2.5069$ , where  $v$  was electric fan wind speed and  $f$  was the frequencies of the fluttering motion calculated using FFT. It was critical for the practical applications to design the PG structure considering the acquired frequency–velocity relationship.

The output current of the PG was also measured under the wind speed in the range of 3.48-12.25 m/s as depicted in Figure S3 of Supporting Information and the wind speed dependent fluttering motion and associated frequencies was measured to follow a similar trend as the output voltage. Wind speed dependent performance of the PG for both the current and the voltage showed a consistent tendency such that the measured maximum outputs were over 100 nA and 1.2 V, respectively, as shown in Figure S4 a-b.

**Table 1** Velocity–frequency relationship

Velocity[m/s]	3.41	5.78	7.45	11.39
Frequency[Hz]	5	17	22	50

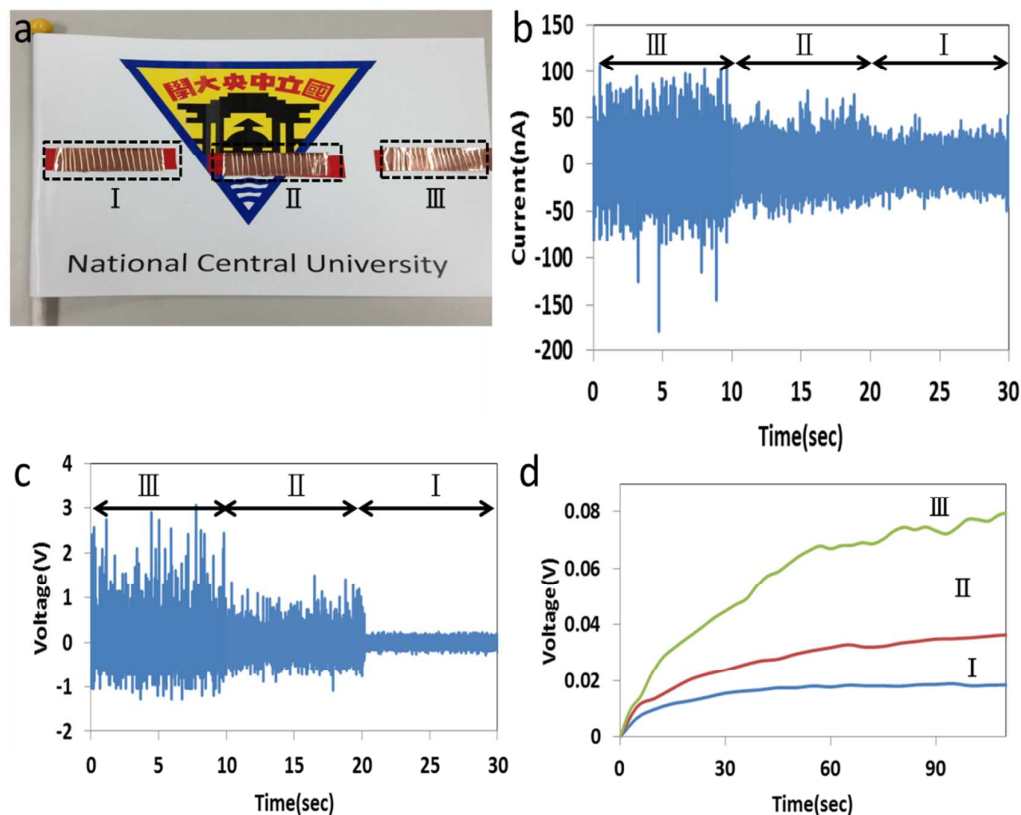


Figure 3 Position-dependent performance of the flexible, energy harvesting PG under waving motion. (a) Three PGs attached at different positions (I, II, III) of the flag surface. (b) Output current and (c) voltage of the PG at the different positions. (d) Capacitor charging capability as the voltage increases when the PG was connected through a bridge rectifier.

#### 4. PG as an energy harvesting device

Position-dependent performance of the flexible, energy harvesting PG from a waving flag was explored. The same PG was attached at different positions of the flag surface under the same experimental conditions, as shown in Figure 3a. The device was firmly fixed on the flag surface and the electric fan was employed to simulate the wind condition. Figures 3b-c show the measured output current and voltage at different positions, corresponding to I, II, III in Figure 3a. It was reasonable to deduce that the output was in the descending order of position I, II, III, respectively since the fixed end was close to position I and the waving displacement was the minimum. Therefore, the output performance was highly dependent on the position as well as the frequency and amplitude of the vibration of the flag. Subsequently, the available electricity and conversion from the wind was explored by connecting a 2.2  $\mu\text{F}$  capacitor to the PG through a bridge rectifier. The increasing voltage curves for a

practical direct current (DC) power source are shown in Figure 3d. Again the position-dependent charging performance from the PG is demonstrated as function of position, and is evident from the faster charging speed of the capacitor. We also investigated the performance enhancement using a novel elongated structure to harvest the full fluttering motion under various air-flow velocities as shown in Figure S5 of Supporting Information. For the detail calculation of Output power and conversion efficiency of a typical NFES NFs based PVDF device as well as Long-term stability tests are provided in Figure S6-7 of Supporting Information.

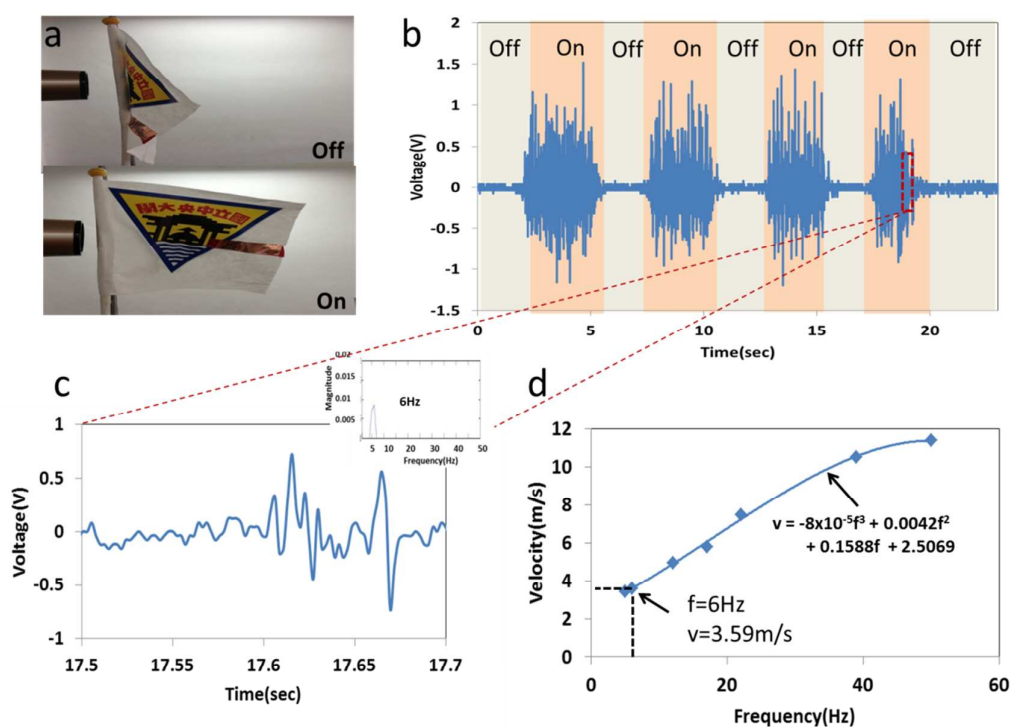


Figure 4 Characterization of the PG frequency-velocity curve induced from ambient wind-speed measurement. (a) Photographs of the electric fan in the on and off state. (b) Corresponding voltage output. (c) Magnified output curve from 17.5 s to 17.7 s. The inset shows the frequency spectrum and the fluttering frequency was identified as 6Hz. (d) Frequency–velocity curve for wind speed from 0 to 11.4m/s.

## 5. Measurement of ambient wind condition

The characterization and experimental setup of the PG frequency-velocity curve induced from ambient wind-speed measurement are shown in Figure 4a. The output of electric fan in parallel at ~3cm to the front face of the flag. Experimentally, two

working conditions, i.e. on or off state can be controlled by turning the switch. Figure 4b shows the output under these conditions. When the electric fan was turned off, the PG output was less than 10 mV, which was basically from the system noise reported before<sup>20</sup>. Experimentally, the output voltage increases and reaches a maximum value of 1.5V when the electric fan was turned on, which was almost five-fold increase compared to ZnO nanowire based PG. The sudden fluttering motion induced random signals can be attributed mainly to the instantaneous pressure change of induced air-flow around the PG. After the initial unsteady state, the output voltage gradually reaches a stable stage and fluctuates in the range of -1V to 1V. The output returns to the noise of 10 mV when the electric fan was off again, indicating the output was indeed from the interaction between air-flow and flag. FFT analysis of the output signal was used to characterize the fluttering frequency of the flag due to induced air-flow. The voltage output from 17.5 s to 17.7 s. and its spectrum are shown in Figure 4c and the inset, respectively. The main fluttering frequency was filtered and calculated to be about 6 Hz. By substituting the frequency into the previously obtained frequency–velocity curve, the transient wind-velocity was obtained as 3.59 m/s besides in the ambient wind-velocity measurement as shown in Figure 4d.

## 6. Conclusions

In summary, we have successfully fabricated a highly flexible and substrate-independent piezoelectric PG based on near-field electrospun NMF and cost-effective thin metal electrode. Utilizing the direct-write technique to align piezoelectric PVDF NMF in preferential direction and the unique properties of in-situ mechanical stretching and electrical poling, the flexible PG can harvest energy from a PG-attached flag in a light-to-medium wind condition (wind speed from 0 to 11.4m/s). When the wind speed increases, the frequency and performance improves. Instead of the previously reported composite design using two kinds of piezoelectric materials (ZnO and PVDF)<sup>20</sup>, we use only a single material system with a very small form factor, that is highly flexible and yet simple in construction. In addition, the proposed active deformation sensor has been successfully deposited on four different flexible substrate materials, indicating the superior and versatile capability of NFES in depositing substrate-independent NMF arrays. As a demonstration, the PG-attached flag exhibits super-flexible and excellent conformability such that the dual functionality of a self-powered sensor and an energy harvesting device is successfully implemented under the waving motion. We believe that this is a landmark progress for NFES type self-powered sensors and can be extremely beneficial as well as

supplemental to the widely used ZnO-based devices that require specific nano-transfer and assembly techniques.

## References

- 1 G. Zhu, R. Yang, S. Wang, and Z. L. Wang, *Nano Lett.*, 2010, 10, 3151-3155.
- 2 Y. Qin, X. Wang and Z. L. Wang, *Nature.*, 2008, 451, 809-813.
- 3 R. Yang, Y. Qin, L. Dai, Z. L. Wang, *Nat. Nanotechnol.*, 2009, 4, 34-39.
- 4 S. Xu, Y. Qin, C. Xu, Y. Wei, R. Yang, Z. L. Wang, *Nat. Nanotechnol.*, 2010, 5, 366-373.
- 5 Y. Hu, Y. Zhang, C. Xu, L. Lin, R. L. Snyder, and Z. L. Wang, *Nano Lett.*, 2011, 11, 2572-2577.
- 6 M. Lee, J. Bae, J. Lee, C. S. Lee, S. Hong and Z. L. Wang, *Energy Environ. Sci.*, 2011, 4, 3359-3363.
- 7 Z. L. Wang, J. Song. *Science.*, 2006, 312, 242-246.
- 8 X. Chen, S. Xu, N. Yao and Y. Shi, *Nano Lett.*, 2010, 10, 2133-2137.
- 9 Z. H. Lin, Y. Yang, J. M. Wu, Y. Liu, F. Zhang, and Z. L. Wang, *J. Phys. Chem. Lett.*, 2012, 3, 3599-3604.
- 10 C. Chang, V. H. Tran, J. Wang, Y. K. Fuh and L. Lin, *Nano Lett.*, 2010, 10, 726-731.
- 11 D. Sun, C. Chang, S. Li, L. Lin, *Nano Lett.*, 2006, 6, 839-842.
- 12 C. Chang, K. Limkraisiri, L. Lin, *Appl. Phys. Lett.*, 2008, 93, 123111-1.
- 13 S. Lee, S-H. Bae, L. Lin, Y. Yang, C. Park, S-W. Kim, S. N. Cha, H. Kim, Y. J. Park, and Z. L. Wang, *Adv. Mater.*, 2012, Online, DOI: 10.1002.
- 14 M. Lee, C-Y. Chen, S. Wang, S. N. Cha, Y. J. Park, J. M. Kim, L-J. Chou, and Z. L. Wang, *Adv. Mater.*, 2012, 24, 1759-1764.
- 15 A. Yu, P. Jiang and Z. L. Wang, *Nano Energy.*, 2012, 1(3), 418-423.
- 16 S. N. Cha, S. M. Kim, H. J. Kim, J. Ku, J. I. Sohn, Y. J. Park, B. G. Song, M. H. Jung, E. K. Lee, B. L. Choi, J. J. Park, Z. L. Wang, J. M. Kim and K. Kim, *Nano Lett.*, 2011, 11, 5142-5147.
- 17 X. Wang, J. Song, J. Liu, Z. L. Wang, *Science.*, 2007, 316, 102-105.
- 18 Z. T. Li and Z. L. Wang, *Adv. Mater.*, 2011, 23, 1.
- 19 Y. Hu, C. Xu, Y. Zhang, L. Lin, R. L. Snyder and Z. L. Wang, *Adv. Mater.*, 2011, 23(35), 4068-4071
- 20 R. Zhang, L. Lin, Q. Jing, W. Wu, Y. Zhang, Z. Jiao, L. Yan, Ray P. S. Han and Z. L. Wang, *Energy Environ. Sci.*, 2012, 5, 8528-8533.
- 21 C. Sun, J. Shi, D. J. Bayerl, X. Wang, *Energy Environ. Sci.*, 2011, 4, 4508-4512.
- 22 Y. K. Fuh, S. Y. Chen, J. C. Ye, *Appl. Phys. Lett.*, 2013, 103, 033114.
- 23 Zhong Lin Wang and Wenzhuo Wu, *Angew. Chem. Int. Ed.*, 2012, 51, 11700 -

11721.

24 Wenzhuo Wu, Xiaonan Wen, Zhong Lin Wang, *Science.*, 2013, 340, 952-957.